Photoinduced electron transfer processes in oligothiophene/C60 composite films

The adsorption of CO on Rh(100): Reflection absorption infrared spectroscopy, low energy electron diffraction, and thermal desorption spectroscopy

A. M. de Jong and J. W. Niemantsverdriet[a)]
Schuit Institute of Catalysis, Eindhoven University of Technology, 5600 MB Eindhoven, The Netherlands

(Received 3 August 1994; accepted 1 September 1994)

The adsorption of CO on Rh(100) has been investigated as a function of temperature and CO pressure, with reflection absorption infrared spectroscopy (RAIRS), low energy electron diffraction (LEED), and thermal desorption spectroscopy (TDS). At low coverages, most CO adsorbs linearly, up to 0.5 monolayers (ML), where a $c(2\times2)$ LEED pattern is observed. The saturation coverage at 300 K is 0.75 ML, associated with a $p(4\sqrt{2}\times\sqrt{2})R45°$ LEED pattern, and adsorption of CO in at least three states, namely two linear modes and one bridged mode. At temperatures well below 300 K and relatively high exposures, CO is compressed into a dense hexagonal overlayer structure with a $c(6\times2)$ LEED pattern and a saturation coverage of 0.83 ML, in which the majority of the CO is bonded linearly. The activation energy of desorption for CO from Rh(100) in the limit of zero coverage is 131 ± 4 kJ/mol and the preexponential factor is $(4\pm3)\times10^{16}$ s^{-1}. We compare our results with the literature of CO on Rh(100), which shows contradictory results on the vibrational spectra, LEED structures, and saturation coverages of CO. © *1994 American Institute of Physics.*

I. INTRODUCTION

Although the adsorption of CO on catalytically relevant surfaces has been studied for a long time, there is still uncertainty on the vibrational properties of this molecule on single crystal surfaces of several transition metals, e.g., rhodium. Reflection absorption infrared spectroscopy (RAIRS) allows for a highly accurate determination of the vibrational characteristics of CO on metals under a wide range of pressures. We have used this technique to study the adsorption of CO on the Rh(100) surface.

A RAIRS study of CO on Rh(100) by Leung *et al.*[1] indicates that CO adsorbs at all coverages in linear and bridged modes. This work, however, disagrees with previous electron energy loss spectroscopy (EELS) studies by Gurney *et al.*[2] and by Richter *et al.*[3] who observed that CO occupies mainly linear adsorption sites at low coverages, up to 0.5 monolayer (ML), while the bridged mode appeared in addition at higher coverages. Although RAIRS has a significantly higher resolution than standard EELS and accordingly reveals more detail, there is no doubt that bridged CO species as seen by Leung *et al.*[1] should have shown up in the EELS spectra.

With respect to overlayer structure, all authors agree that CO forms a $c(2\times2)$ structure at low coverages, but various structures are mentioned for higher CO coverages. Tucker[4] assigned a low energy electron diffraction (LEED) pattern that with hindsight corresponds to a $p(4\sqrt{2}\times\sqrt{2})R45°$ structure to a coincidence lattice of CO on Rh(100). Several authors[1,2,5] report to have observed the $p(4\sqrt{2}\times\sqrt{2})R45°$ structure at a saturation coverage of 0.75 ML. Indeed, Biberian and van Hove[6] have shown that the formation of $p(n\sqrt{2}\times\sqrt{2})R45°$ overlayer lattices with $n=2,3,...,7$ is a general feature of CO adsorption on the (100) surfaces of face-centered-cubic (fcc) metals. Castner *et al.*[7] describe the formation of a "split" (2×1) structure, in which CO orders hexagonally, observed at a coverage of 0.83 ML.

Thermal desorption studies of CO from Rh(100) have been reported by Kim *et al.*,[5] who find an activation energy of desorption of 134 kJ/mol and a pre-exponential factor of 8.4×10^{12} s^{-1} in the limit of zero coverage, as determined by Chan's method.

A comparison between the different studies is not always possible because of the different conditions used. The purpose of our investigation has been to study the adsorption of CO on Rh(100) as a function of coverage and at different temperatures. If we adjust the coverage calibration employed by Kim *et al.*,[5] our results reconcile most of the work of Tucker,[4] Castner *et al.*[7], Kim *et al.*,[5] and Ho and co-workers,[2,3] but do not confirm all the results reported by Leung *et al.*[1]

II. EXPERIMENT

The work has been done with a home-built RAIRS system as drawn schematically in Fig. 1. It consists of an ultra-high vacuum(UHV) chamber and a separate cell to perform RAIRS. The sample is transferred between the two by a magnetically driven transfer rod. The main chamber houses a reverse view four grid Auger electron spectroscopy (AES)/LEED system (Spectaleed, Omicron Vakuumphysik), and a quadrupole mass spectrometer (Quadruvac Q100, Leybold) for TDS analysis, as well as an argon ion gun (AS-10, VSW) for sputter cleaning. The system is pumped by a 360 ℓ/s turbomolecular pump and a water-cooled titanium sublimation pump (Leybold). The base pressure after bakeout is typically 2×10^{-10} mbar.

The RAIRS cell has a spherical shape on the inside in order to allow optimum space for sample manipulation. The cell contains two KBr windows mounted in differentially pumped holders. It can be isolated from the main chamber by a gate valve (VAT) for experiments at pressures up to 1 bar,

a)Corresponding author.

 0021-9606/94/101(11)/10126/8/$6.00

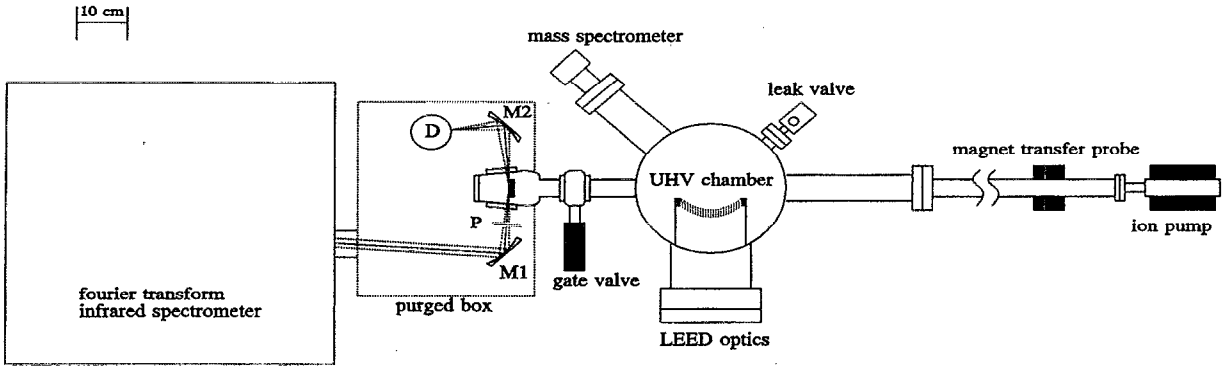

FIG. 1. A schematic drawing of the RAIRS apparatus, showing the UHV chamber and the RAIRS cell and optics. The parabolic mirror $M1$ focuses the infrared beam on the sample through a KRS-5 wire grid polarizer (P). The reflected beam is collected by a parabolic mirror $M2$, which focuses the beam directly on the MCT detector (D).

and can be separately pumped by a 150 ℓ/s turbomolecular pump. Both the UHV chamber and the RAIRS cell are fitted with vertically mounted $xyz\theta$ manipulators with differentially pumped rotary feedthroughs and liquid nitrogen cold fingers. The sample manipulation and transfer system is a slightly modified version of the one published by Raval *et al.*[8] The single crystal is resistively heated by two tantalum support wires of 0.25 mm diameter, pressed in slots at the sides of the crystal. The temperature is monitored with a chromel–alumel thermocouple. This configuration allows cooling to 140 K and heating to 1300 K.

The RAIRS cell is optically interfaced (Fig. 1) with a Fourier transform infrared spectrometer (Galaxy 4020, Mattson) in a way that the infrared beam undergoes a single reflection from the crystal surface at near grazing incidence (85°) required for the RAIRS experiment.[9] The infrared beam falls on a KRS-5 wire grid polarizer (P) and is focused on the sample by a parabolic mirror ($M1$). The reflected beam is collected by a second parabolic mirror ($M2$), which focuses it directly on the detector (D). We use a liquid nitrogen cooled narrow band mercury cadmium telluride (MCT) detector, which allows the spectral range from 4000 to 800 cm^{-1} to be accessed. The entire optical path outside the UHV is flushed with dry nitrogen to reduce fluctuations in the spectra by absorption bands of atmospheric CO_2 and H_2O.

The crystal was initially cleaned by extensive heating in 2×10^{-7} mbar oxygen at 870 K to remove carbon contaminations. Phosphor, sulphur, boron, and chlorine contaminations were eliminated by sputter/anneal cycles till these contaminants depleted from the surface region. Sputtering was done with 500 eV Ar^+ ions. Routinely, the crystal was cleaned by two cycles of sputtering for 20 min, followed by flashing to 1100 K. Then the sample was heated at 870 K in 2×10^{-7} mbar oxygen for 20 min and flashed to 1200 K. After this cleaning procedure, Auger spectra did not show any contamination. The surface structure was checked with LEED, which showed a sharp $p(1\times1)$ pattern. The shape and position of CO desorption peaks were used as the final test to check the surface cleanliness, since CO desorption is much more sensitive to trace impurities on the surface than AES is.

LEED data were obtained with an electron beam current between 10 and 20 μA. Photographs were made with a 3200 asa film and 1/8 or 1/15 s exposure time. After each high pressure exposure, the gas phase was pumped off before the LEED experiments were carried out. Thermal desorption spectra were recorded by linearly ramping the crystal temperature at a rate of 3.5 K/s, with the normal of the crystal surface directed to the mass spectrometer. Gas exposures were made by backfilling the chamber with a leak valve, up to pressures of 1×10^{-8} mbar, unless indicated otherwise. For the CO adsorption experiments, we used 99.997 vol.% pure carbon monoxide (CO4.7, Messer Griesheim).

The RAIRS spectra were recorded at an instrumental resolution of 4 cm^{-1} and by adding 400 interferometer scans. Such a spectrum was recorded in about 100 s. Before all experiments were done, first a background spectrum of 400 scans was recorded of the clean sample. The spectra were ratioed to this background spectrum of the clean surface.

III. RESULTS

A. Low energy electron diffraction

Three characteristic LEED patterns appeared in our study (they are shown in Fig. 2). Adsorption of CO at 300 K at exposures up to 1.5 L results in the $c(2\times2)$ pattern, as reported by several authors.[1,2,5,7] At higher exposures, the $c(2\times2)$ pattern goes over in the $p(4\sqrt{2}\times\sqrt{2})R45°$ structure observed by others.[2–5] The open squares in Fig. 2(b) denote spots that could only be observed with non-normal incidence of the primary electron beam. This structure persists even at high exposures, i.e., 100 s at 1×10^{-6} mbar, indicating that the $p(4\sqrt{2}\times\sqrt{2})R45°$ overlayer structure is associated with the saturation coverage of CO at room temperature. Upon heating, $p(4\sqrt{2}\times\sqrt{2})R45°$ transforms to the $c(2\times2)$ pattern at about 340 K. Above 400 K, the $c(2\times2)$ structure becomes

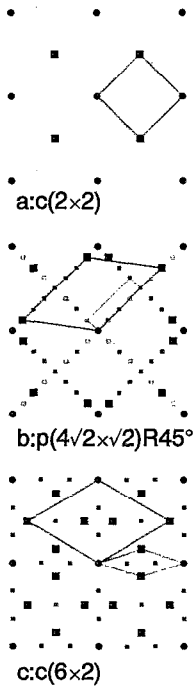

FIG. 2. LEED patterns observed at different exposures and temperatures. The Rh substrate spots are denoted by the solid circles (●). The large solid squares (■) represent intense overlayer spots, the small solid squares (▪) represent weak overlayer spots, and the open squares (□) represent missing spots, only observed at off-normal incidence. (a) $c(2\times2)$ pattern at 0.5 ML coverage; (b) $p(4\sqrt{2}\times\sqrt{2})R45°$ pattern at 0.75 ML coverage; (c) $c(6\times2)$ pattern, observed after exposure to 1×10^{-6} mbar CO at 220 K. The solid lines represent the unit cells according to the compact model; the dashed lines represent the coincidence unit cells.

faint and disappears gradually until at 500 K only the $p(1\times1)$ pattern of the Rh(100) substrate remains. Adsorption of CO at 370 K results in the $c(2\times2)$ pattern, which remains until saturation.

High exposures of 1×10^{-6} mbar CO for 100 s at 220 K result in the pattern of Fig. 2(c). This pattern is very similar to the one Castner *et al.*[7] observed and designated as a "split"(2×1) structure. These authors, however, did not observe the low intensity spots denoted by the small squares in Fig. 2(c). Taking these additional spots into account, we assign this LEED pattern to a $c(6\times2)$ structure (see discussion for further detail). Upon heating, $c(6\times2)$ gradually goes over into the $p(4\sqrt{2}\times\sqrt{2})R45°$ pattern between 250 and 280 K. At 300 K, only the $p(4\sqrt{2}\times\sqrt{2})R45°$ pattern remains. This process is reversible. If we cool the crystal under exposure to 1×10^{-6} mbar CO, a mixture of the two patterns appears at about 280 K, until at 220 K, only the $c(6\times2)$ pattern is present. Exposing the crystal to 10^{-6} mbar of CO for 100 s at 260 K results again in a $c(6\times2)$ pattern, which transformed slowly into the $p(4\sqrt{2}\times\sqrt{2})R45°$ pattern during the LEED experiment as the CO gas was pumped out.

In conclusion, CO adsorption at low exposures results in a $c(2\times2)$ LEED pattern, which is also the pattern observed for saturation coverage at 370 K. Saturation coverage of CO

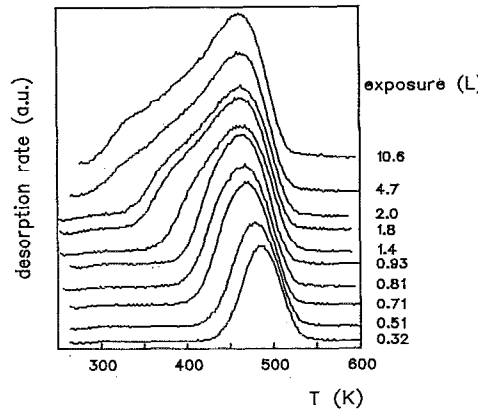

FIG. 3. TDS spectra of CO adsorbed at 300 K for several exposures. The heating rate is 3.5 K/s.

at room temperature corresponds to a $p(4\sqrt{2}\times\sqrt{2})R45°$ pattern, while high CO exposures at temperatures well below room temperature, e.g., 260 K, leads to the formation of a $c(6\times2)$ pattern.

B. Thermal desorption

TDS experiments were done in order to obtain a calibration of coverage versus exposure and to determine the kinetic parameters for the desorption of CO from Rh(100). The set of TDS traces of Fig. 3, obtained after adsorption of CO at 300 K, indicates a single CO adsorption state for low exposures, the development of a low temperature desorption state at coverages above 1 L, and a third at high exposures, ~4.7 and higher. The areas under the spectra, which are proportional to the initial coverage of CO, have been plotted as a function of exposure in Fig. 4. If we set the saturation coverage of CO at 300 K in the $p(4\sqrt{2}\times\sqrt{2})R45°$ structure at 0.75 ML, as proposed by Richter *et al.*, the $c(2\times2)$ structure, which saturates at about 1.5 L, is seen to correspond to a coverage of 0.5 ML, as expected.

The TDS spectra obtained for CO coverages up to 0.5 ML exhibit a single CO adsorption state. The shift of this peak to lower temperatures suggests that repulsive interactions between the adsorbed CO molecules are present. Application of the Chan–Aris–Weinberg method for TDS analysis yields an activation energy of desorption of 131 ± 4 kJ/mol and a preexponential factor of $(4\pm3)\times10^{16}$ s^{-1} in the limit of zero coverage.[10,11]

Figure 4 indicates that the adsorption of CO can be described with the precursor model of Kisliuk,[12] in which the sticking coefficient is given as

$$S(\theta)=S_0\,\frac{1-\theta}{1+(K-1)\theta}. \tag{1}$$

$S(\theta)$ is the sticking coefficient as function of the coverage, S_0 is the initial sticking coefficient, θ is the adsorbate coverage, and K is the precursor state parameter. Note that $K=1$ corresponds to direct adsorption, as predicted by the Langmuir isotherm. The CO uptake is thus described by

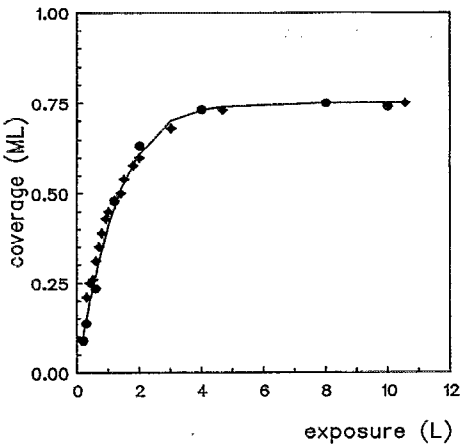

FIG. 4. Coverage as a function of the CO exposure, obtained from two series of TDS spectra of CO adsorbed at 300 K represented by diamonds and circles. The solid line shows the uptake curve, derived from the model after Kisliuk (Ref. 12), describing precursor kinetics, with $\alpha S_0=0.75$ and $K=0.7$.

$$\frac{d\theta}{dt}=\alpha S(\theta)p_{CO}=\alpha S_0 p_{CO}\frac{1-\theta}{1+(K-1)\theta}, \qquad (2)$$

where the factor α has been introduced to account for the calibration of the pressure meter, which is not accurately known. The solid line in Fig. 4 has been calculated by integrating Eq. (2) numerically with values of $K=0.7$ and $\alpha S_0=0.75$.

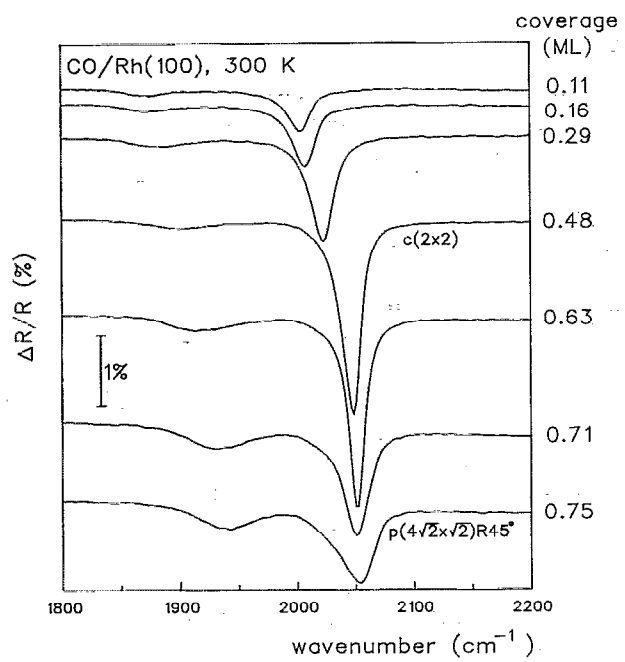

FIG. 5. RAIRS spectra of CO adsorbed on Rh(100) at 300 K, for different CO coverages.

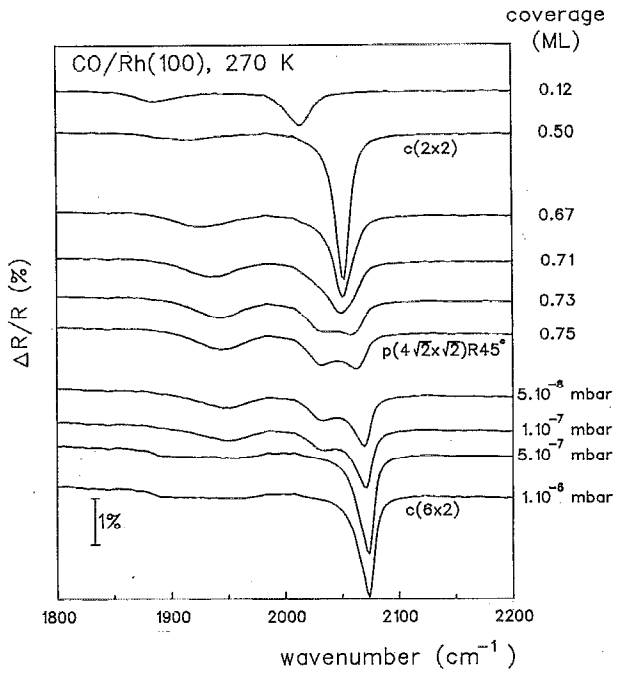

FIG. 6. RAIRS spectra of CO adsorbed on Rh(100) at 270 K for different CO coverages up to 0.75 ML and at higher CO pressures.

C. Reflection absorption infrared spectroscopy

RAIRS experiments were done at several temperatures and CO exposures. Figures 5 and 6 show the spectra of CO adsorbed on Rh(100) as a function of CO coverages at 300 and 270 K, respectively. After each RAIRS spectrum, thermal desorption was applied to determine the coverage. All frequencies have been collected as a function of coverage in Fig. 7. Figure 8 displays the integrated absorption intensities as a function of coverage.

For coverages up to 0. 5 ML, the spectra almost exclusively consist of one infrared peak characteristic of linearly adsorbed CO with a coverage dependent frequency, shifting from about 2000 cm^{-1} for CO on the empty surface to 2052 cm^{-1} for CO in the $c(2\times2)$ geometry. We attribute the contribution around 1875 cm^{-1} to a small amount of bridged CO. The absorption intensity of the linear CO band increases strongly with coverage up to 0.5 ML. Concomitantly, the peak narrows with increasing coverage till at 0.5 ML the band is highly symmetric and narrow. We conclude that the $c(2\times2)$ adsorption geometry of CO on Rh(100) is associated with a linear CO species and a vibrational frequency of 2052 cm^{-1}.

If the coverage of CO is increased above 0.5 ML, bridged sites get increasingly occupied, as revealed by a peak shifting from 1910 cm^{-1} at 0.5 ML to 1944 cm^{-1} at 0.75 ML. At coverages between about 0.7 and 0.75 ML, a second peak characteristic of linear CO grows in. This peak is best resolved in the spectra at 270 K, but is also present at room temperature. The integrated absorption intensity of the bridged CO band increases from 0.5 ML to saturation coverage, while simultaneously the band of linear CO decreases in

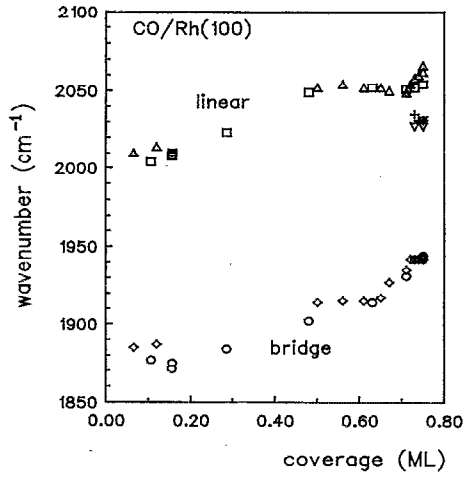

FIG. 7. The CO stretch frequencies as a function of the coverage of CO adsorbed on Rh(100) at 270 (△—linear, ◇—bridge, +—low frequency linear peak) and 300 K (□—linear, ○—bridge, ▽—low frequency linear peak) in the coverage range up to 0.75 ML.

intensity. In summary, CO adsorbed in the $p(4\sqrt{2}\times\sqrt{2})R45°$ geometry is present in three different states with vibrational frequencies of 2054, 2031, and 1944 cm^{-1}.

Spectra taken at 270 K under higher CO pressures (Fig. 6) show that the highest frequency peak of linear CO gains intensity and shifts to higher frequencies. At saturation, obtained under 10^{-6} mbar of CO, the spectrum consists of a sharp, highly intense peak of linear CO with a frequency of 2074 cm^{-1} and a very broad signal between 1880 and 1970 cm^{-1} in the range of bridged CO. As argued above, we believe that this spectrum is representative for the $c(6\times2)$ adsorption geometry. Heating under 10^{-6} mbar to 300 K results in the spectrum characteristic of the $p(4\sqrt{2}\times\sqrt{2})R45°$ structure, while recooling to 270 K restores the original spectrum measured at 270 K. RAIRS spectra at 270 K obtained after pumping away CO indicated that the intense linear CO band lost some intensity, while the second linear as well as the bridged CO species reappeared to some extent, indicating that both the $c(6\times2)$ and the $p(4\sqrt{2}\times\sqrt{2})R45°$ structures are present.

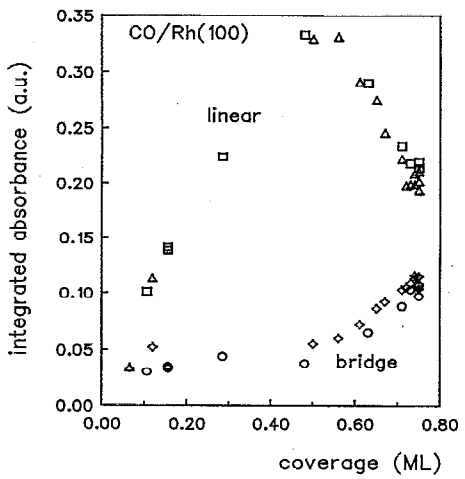

FIG. 8. Integrated absorption intensities of the CO bands as a function of coverage for CO adsorbed on Rh(100) at 270 (△—linear, ◇—bridge) and 300 K(□—linear, ○—bridge) in the coverage range up to 0.75 ML. The intensity of the linear peak represents the total intensity of both linear species.

TABLE I. Characteristic data on the adsorption of CO on Rh(100).

Coverage (ML)	Adsorption state	Frequency (cm^{-1})	Structure	Remarks
$\theta\simeq0$	Linear	1995	···	$E_{des}\simeq131$ kJ/mol $\nu_{des}\simeq4\times10^{16}$ s^{-1}
$\theta=0.5$	Linear	2052	$c(2\times2)$	Saturation coverage at 370 K
$\theta=0.75$	Linear	2054 2031	$p(4\sqrt{2}\times\sqrt{2})R45°$	Saturation coverage at 300 K
	Bridge	1944		
$\theta=0.83$	Linear	2074	$c(6\times2)$	Saturation coverage below 280 K at CO pressures above 5×10^{-7} mbar
	Bridge	1880–1970		

IV. DISCUSSION

The combination of LEED, TDS, and RAIRS gives detailed insight into the adsorption of CO on Rh(100). There are three different coverage regions, as summarized in Table I. We will compare our results with those reported in the literature.

A. CO coverage between 0 and 0.5 ML

There is general agreement that CO forms a $c(2\times2)$ overlayer at 0.5 ML coverage.[1,2,5,7] For coverages up to 0.5 ML, the TDS spectra indicate a single desorption peak, corresponding to one adsorption state of CO, which is in agreement with results reported by Kim *et al.*[5] The RAIRS spectra show that CO is linearly coordinated, as was also reported by Gurney *et al.*[2] and Kao *et al.*[13] on the basis of EELS experiments. Linear adsorption has also been observed for low CO coverages on the (111) surface of rhodium.[14–16] The RAIRS results of Leung *et al.*[1] for CO adsorbed on Rh(100) at 300 K, however, show, in contrast to the mentioned EELS results and the present RAIRS experiments, a high contribution of bridged CO species.

It is useful to mention that bridged CO species also appeared in the course of our work. In such cases, however, several facts indicated the presence of a surface (or near-surface) contamination, although no other elements than rhodium were detected with AES. First, the IR absorption peaks showed some asymmetry and were slightly broadened in comparison with the spectra of Fig. 5, indicating that the CO adlayer was to some extent disturbed. Second, the intensity of the absorption band was lower than in Fig. 8, while TDS showed that the saturation coverage of 0.75 ML at room

temperature could not be reached. Third, the desorption peak had shifted to lower temperature, suggesting a more weakly bound CO species. We therefore believe that the appearance of significant amounts of bridged CO species at coverages below 0.5 ML is indicative of impurities on the surface. In this respect, it is relevant to note that coadsorption of, e.g., hydrogen also leads to the appearance of bridged bonded CO.[3] In short, we think that the results obtained by Leung *et al.*[1] on the adsorption of CO on Rh(100) at 300 K have been obtained in the presence of an undetected impurity. This would also explain why these authors measured a saturation coverage for CO at 300 K of 0.6 instead of 0.75 ML. There is no disagreement between the results Leung *et al.*[1] report at low temperature and the work described by Gurney *et al.*[2] and by us.

The shift in frequency as well as the nonlinearly increasing integrated absorption intensity of the CO absorption band as a function of coverage between 0 and 0.5 ML, shown in Figs. 7 and 8, can be explained entirely by dipole–dipole interactions in the model of Persson and Ryberg.[17] Screening, due to the electronic polarizability of the adsorbed molecules, reduces both the frequency shift and the absorption intensity. The center frequency and the area of the adsorption band depend on coverage as[17]

$$\left(\frac{\omega}{\omega_0}\right)^2 = 1 + \frac{\alpha_\nu U\theta}{1+\alpha_e U\theta}, \tag{3}$$

$$\int \frac{\Delta R}{R}\, d\nu = \frac{\alpha_\nu U\theta}{(1+\alpha_e U\theta)^2}, \tag{4}$$

in which ω is the vibrational frequency of the infrared band, ω_0 is the same in the limit of zero coverage (1995 cm^{-1}), ν is the frequency of the infrared light, $\Delta R/R$ is the reflectivity change, θ is the adsorbate coverage, α_ν is the vibrational polarizability of the adsorbed molecule, α_e is its electronic polarizability, and U is the summation term of the dipoles over a $c(2\times2)$ overlayer structure, taking into account the image dipoles of the adsorbed molecules ($U=0.3$ Å^{-3}). Figure 9 shows fits of Eqs. (3) and (4) to the absorption intensity and the frequency of the linear CO peak obtained by varying the polarizabilities; the fits correspond to $\alpha_\eta=0.48$ Å^3 and $\alpha_e=1.8$ Å^3. The Persson and Ryberg model gives an adequate description of the data, confirming that the shift in frequency and the less than linear increase of the band intensity as a function of the coverage can be assigned to dipole coupling, provided that dielectric screening is taken into account.

B. CO coverages between 0.5 and 0.75 ML

Additional adsorption states appear when the CO coverage exceeds that of the $c(2\times2)$ overlayer structure. Between 0.5 and 0.7 ML, there is evidence for a linear and a bridged CO species, in full agreement with the EELS study of Gurney *et al.*[2] Between 0.7 and 0.75 ML, a second linear CO species appears. The latter was not (and could not be) detected by Gurney *et al.*[2] due to the intrinsically lower resolution of the EELS technique. The same reason accounts for the fact that these authors find a higher fraction of CO in bridge sites for the $p(4\sqrt{2}\times\sqrt{2})R45°$ structure than we observe, as the intensity of the second linear CO species was probably included in the intensity of the bridged CO. Consequently, the model that Gurney *et al.*[2] propose for CO in the $p(4\sqrt{2}\times\sqrt{2})R45°$ structure, in which CO is believed to occupy twice as many bridge as top sites, cannot account for our RAIRS spectra.

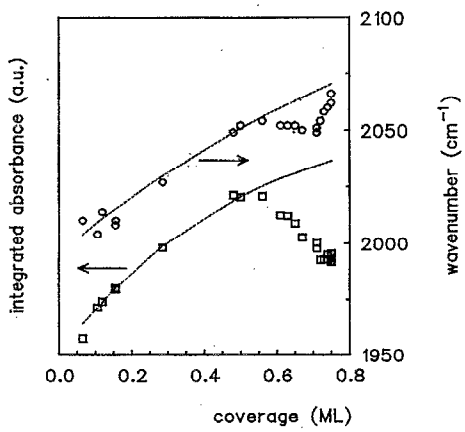

FIG. 9. Integrated absorption intensity (□) and frequency (○) of the linear CO band as a function of the coverage. The dashed lines represent the fits after the model of Persson and Ryberg (Ref. 17).

Not all publications on the CO/Rh(100) system agree on the saturation coverage of CO. We believe that our calibration with a saturation coverage of 0.75 ML of CO at room temperature is correct, because in this calibration, the $c(2\times2)$ LEED pattern appears most clearly at a coverage of 0.5 ML. In addition, the RAIRS spectra still show a narrow single line spectrum of linear CO, while the single adsorption state in TDS is just about to broaden. Setting the saturation coverage for CO on Rh(100) to 0.75 ML at room temperature leads to mutual agreement between the coverages at which characteristic features are observed in almost all studies.[1–3,5] We note that if we recalibrate the results of Peebles *et al.*[18] to a saturation coverage of 0.75 instead of 0.6 ML, the step in the work function change with increasing CO coverage, attributed to a change from linear to bridged bonding, falls at 0.5 ML, in agreement with both the EELS data of Gurney *et al.*[2] and the present RAIRS data.

The compression of the CO overlayer with increasing coverage in structures such as the $p(4\sqrt{2}\times\sqrt{2})R45°$ pattern has been observed for many other metals with a (100) surface orientation, such as Ni, Cu, Pd, and Pt.[6,19] According to Biberian and Van Hove,[6] the $p(4\sqrt{2}\times\sqrt{2})R45°$ LEED pattern can be interpreted in two different ways. In the first approach, it is assumed that the observed LEED patterns are composed of diffraction spots originating from either the substrate or the adsorbate, or from double diffraction between the substrate and the overlayer. Normally, only intense spots are taken into account; other spots are composed of linear combinations of the reciprocal lattice vectors of the substrate and the adsorbate with small (h,k) indices. This interpretation leads to a compact model for the adsorbed CO overlayer, which forms a pseudohexagonal overlayer on the surface. The second approach assumes that there is a coinci-

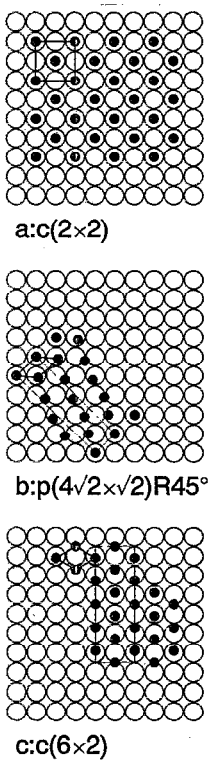

FIG. 10. Models for the CO overlayer structures at (a) 0.5; (b) 0.75; and (c) 0.83 ML coverages.

dence unit cell between the substrate and the overlayer, giving rise to a superstructure. All the spots, not originating from the substrate, are then due to the existence of the coincidence unit cell. Figure 2 shows the two reciprocal unit cells of the $p(4\sqrt{2}\times\sqrt{2})R45°$ LEED pattern. The solid line denotes the reciprocal lattice unit cell, according to the compact model. From this cell, the real space unit cell as depicted in Fig. 10 is derived. Expressing this unit cell in the base vectors of the substrate lattice yields

$$\begin{pmatrix}\mathbf{A}\\ \mathbf{B}\end{pmatrix}=\begin{pmatrix}\frac{1}{6} & 1\\ \frac{7}{6} & -1\end{pmatrix}\cdot\begin{pmatrix}\mathbf{a}\\ \mathbf{b}\end{pmatrix}. \tag{5}$$

The area of this unit cell is 8/6; this means that one CO molecule covers 8/6 coverage of an Rh atom. From this, it follows that the coverage is 0.75 ML. The dashed line in Fig. 2 denotes the coincidence lattice unit cell, resulting in the $p(4\sqrt{2}\times\sqrt{2})R45°$ structure (Fig. 10). It is clear that both methods lead to the same result.

While for coverages up to 0.5 ML, the observed vibrational frequency of CO can straightforwardly be correlated with the adsorption geometry; this is not unequivocally possible in the $p(4\sqrt{2}\times\sqrt{2})R45°$ structure observed at 0.75 ML coverage. Although TDS clearly indicates the presence of more than one CO species, the desorption states are insufficiently resolved for estimating the coverage of the most weakly bound CO species in the $p(4\sqrt{2}\times\sqrt{2})R45°$ structure. Note that the intensities of the species in the RAIRS spectra

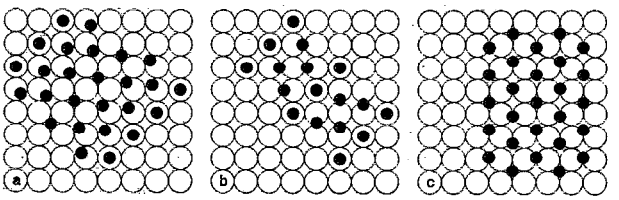

FIG. 11. Real space structures for CO adsorbate layers on Rh(100), (a) Coincidence lattice corresponding to $\theta_{CO}=0.75$ ML proposed by Tucker (Ref. 4); (b) $p(4\sqrt{2}\times\sqrt{2})R45°$ structure ($\theta_{CO}=0.75$ ML) according to Gurney *et al.* (Ref. 2); and (c) the "split" (2×1) structure ($\theta_{CO}=0.83$ ML) proposed by Castner *et al.* (Ref. 7).

(Fig. 8) cannot *a priori* be translated into concentrations because the dynamic dipole moments are unknown. Nevertheless, it is clear that any proposal for the arrangement of CO in the $p(4\sqrt{2}\times\sqrt{2})R45°$ structure will have to account for the presence of three different states of CO.

Figure 11 shows two proposals for the $p(4\sqrt{2}\times\sqrt{2})R45°$ structure as made by Tucker[4] and by Gurney *et al.*[2] Tucker's coincidence structure contains four different adsorption sites for the CO molecule, among which there is a one in fourfold coordination to the rhodium substrate. The latter would give rise to a vibrational absorption band below 1800 cm^{-1}, which, however, is not present in either the EELS spectra of Gurney *et al.*[2] or the present RAIRS spectra. As already noted before, the structure model of Gurney *et al.*[2] does not account for three different CO adsorption sites either.

As an alternative which would be in agreement with all data observed so far, we propose the structure of Fig. 10 in which CO occupies an equal number of linear and bridged sites. According to the IR absorption band intensities in Fig. 8, the ratio of the squares of the dipole moments of the linear and bridged adsorbed CO species would be 1.8, in good agreement with the value of 2.0±0.3 as determined by Gurney *et al.*[2] In this model there are two different types of linear sites in each unit cell, a site with only bridged sites as neighbors and two sites with both bridged and linear sites as neighbors. The tilt of the CO molecules on the former is higher, resulting in more overlap of the $2\pi^*$ orbitals of the CO molecule with the orbitals of the metal substrate, causing the CO stretch frequency to be lower. This distribution of the linear CO species corresponds well with the infrared spectra, which show a higher intensity (about twice as high) of the high frequency linear CO band. We suggest that the model of Fig. 10 is a serious candidate for the $p(4\sqrt{2}\times\sqrt{2})R45°$ structure, as it accounts well for the RAIRS results.

C. CO coverages above 0.75 ML

Exposing the Rh(100) surface to ambient CO pressures of more than 5×10^{-7} mbar and at temperatures well below room temperature, causes a further compression of the CO adsorbate structure in a more densely packed overlayer which gives rise to a $c(6\times2)$ LEED pattern. A similar behavior was observed for the adsorption of CO on the unrecon-

structed Pt(100) surface, after high pressure CO exposures, by Bonzel and co-workers.[20] The $c(6\times2)$ LEED pattern is equivalent to the "split" (2×1) reported by Castner *et al.*[7]

The $c(6\times2)$ pattern can again be interpreted in two different ways. In Fig. 2, the $c(6\times2)$ LEED pattern is shown with the reciprocal lattice unit cells according to the compact model and the coincidence lattice model. The solid line denotes the reciprocal lattice unit cell in the compact model. It corresponds to the real space unit cell depicted in Fig. 10. Expressing this unit cell in the base vectors of the substrate lattice, we obtain

$$\begin{pmatrix} \mathbf{A} \\ \mathbf{B} \end{pmatrix} = \begin{pmatrix} 1 & \frac{3}{5} \\ 1 & -\frac{3}{5} \end{pmatrix} \cdot \begin{pmatrix} \mathbf{a} \\ \mathbf{b} \end{pmatrix}. \tag{6}$$

The area of this unit cell is 6/5, corresponding to a CO coverage of 0.83 ML, in agreement with Castner *et al.*[7] The dashed line in Fig. 10 denotes the coincidence lattice unit cell, resulting in the $c(6\times2)$ structure.

The adsorbate structure proposed by Castner *et al.*[7] (see Fig. 11) involves CO on multiple adsorption sites. The RAIRS spectra of Fig. 6, however, indicate that CO is mainly bound on linear sites. If we shift the overlayer proposed by Castner *et al.*[7] as indicated in Fig. 10, we obtain a configuration in which most of the CO molecules coordinate to a single rhodium atom. Each unit cell contains two CO molecules in a bridged configuration and eight CO molecules in a linear configuration. We propose that the CO molecules on linear sites are tilted to obtain equal distances between the CO molecules in the long direction of the unit cell. The distance between the CO molecules in this overlayer structure is about 3.2 Å. Small intermolecular distances of compressed CO overlayers have been reported earlier for several transition metals.[6,14] The relative intensity observed with RAIRS for the linear and bridged bonded CO is about 7. Since CO occupies four times as much linear as bridged sites, this again yields a ratio of the square of the dynamic dipole moments of 1.8.

In this study, no evidence was found for the presence of *gem*-dicarbonyl species as reported in many studies of the CO adsorption on alumina supported Rh catalysts.[21–24] However, other experiments at CO pressures in the range of 1–150 mbar did reveal the formation of Rh–dicarbonyl species.[25] The formation of $Rh(CO)_2$ species was also observed by Kruse[26] on Rh field emitter tips.

V. CONCLUDING REMARKS

The population of CO in different adsorption sites on Rh(100) was studied as a function of coverage, temperature, and CO pressure. The results are briefly summarized in Table I. On adsorption, CO initially occupies linear adsorption sites, till 0.5 ML coverage, where a $c(2\times2)$ structure is formed. With increasing coverage, the $c(2\times2)$ structure transforms into a $p(4\sqrt{2}\times\sqrt{2})R45°$ structure, in which CO occupies equal numbers of linear and bridged adsorption sites. The CO coverage, when this structure occurs, is 0.75 ML. Applying high CO pressures, the overlayer is further compressed into a highly symmetric $c(6\times2)$ structure, with CO occupying four times as much linear as bridged adsorption sites and a coverage of 0.83 ML. This compressed structure is not formed at CO pressures lower than 5×10^{-7} mbar, even at low temperatures.

It appears that in the adsorption mechanism of CO, a mobile precursor state is involved. The activation energy for desorption at low coverages is about 131 kJ/mol and the preexponential factor for desorption is in the range of 4×10^{16} s^{-1}.

ACKNOWLEDGMENTS

The authors are most grateful to Dr. R. Raval, Dr. S. Haq, and Professor D. A. King for valuable advice on the construction of our RAIRS equipment, and to Ir. P. Brinkgreve and T. M. Maas and co-workers for invaluable technical support. We thank Miss M. van Rij for her assistance in the measurements. This work was supported through grant PGS 70-154 from The Netherlands Organization for Scientific Research (NWO, PGS 70-154).

[1] L.-W. H. Leung, J.-W. He, and D. W. Goodman, J. Chem. Phys. **93**, 8328 (1990).
[2] B. A. Gurney, L. J. Richter, J. S. Villarrubia, and W. Ho, J. Chem. Phys. **87**, 6710 (1987).
[3] L. J. Richter, B. A. Gurney, and W. Ho, J. Chem. Phys. **86**, 477 (1987).
[4] C. W. Tucker, J. Appl. Phys. **37**, 3013 (1966).
[5] Y. Kim, H. C. Peebles, and J. M. White, Surf. Sci. **114**, 363 (1982).
[6] J. P. Biberian and M. A. van Hove, Surf. Sci. **118**, 443 (1982).
[7] D. G. Castner, B. A. Sexton, and G. A. Somorjai, Surf. Sci. **71**, 519 (1978).
[8] R. Raval, M. A. Harrison, and D. A. King, J. Vac. Sci. Technol. A **9**, 345 (1991).
[9] R. G. Greenler, J. Chem. Phys. **44**, 310 (1966).
[10] C.-M. Chan, R. Aris, and W. H. Weinberg, Appl. Surf. Sci. **1**, 360 (1978).
[11] A. M. de Jong and J. W. Niemantsverdriet, Surf. Sci. **223**, 355 (1990).
[12] P. Kisliuk, J. Phys. Chem. Solids **3**, 95 (1957).
[13] C.-T. Kao, C. M. Mate, G. S. Blackman, B. E. Bent, M. A. van Hove, and G. A. Somorjai, J. Vac. Sci. Technol. A **6**, 786 (1988).
[14] M. A. van Hove, R. J. Koestner, J. C. Frost, and G. A. Somorjai, Surf. Sci. **129**, 482 (1983).
[15] L. H. Dubois and G. A. Somorjai, Surf. Sci. **91**, 514 (1980).
[16] T. W. Root, G. B. Fisher, and L. D. Schmidt, J. Chem. Phys. **85**, 4687 (1986).
[17] B. N. J. Persson and R. Ryberg, Phys. Rev. B **24**, 6954 (1981).
[18] D. E. Peebles, H. C. Peebles, and J. M. White, Surf. Sci. **136**, 463 (1984).
[19] S. Andersson, Surf. Sci. **202**, 167 (1988).
[20] G. Brodén, G. Pirug, and H. P. Bonzel, Surf. Sci. **72**, 45 (1978).
[21] S. D. Worley, C. A. Rice, G. A. Mattson, C. W. Curtis, J. A. Guin, and A. R. Tarrer, J. Chem. Phys. **76**, 20 (1982).
[22] H. F. J. Van't Blik, J. B. A. D. Van Zon, T. Huizinga, J. C. Vis, D. C. Koningsberger, and R. Prins, J. Phys. Chem. **87**, 2264 (1983).
[23] P. Basu, D. Panayotov, and J. T. Yates, Jr., J. Am. Chem. Soc. **110**, 2074 (1988).
[24] D. K. Paul, T. H. Ballinger, and J. T. Yates, Jr., J. Phys. Chem. **94**, 4617 (1990).
[25] A. M. De Jong, thesis, 1994.
[26] N. Kruse, J. Vac. Sci. Technol. A **8**, 3432 (1990).